

A Unified Jet Model of X-Ray Flashes and Gamma-Ray Bursts

D. Q. Lamb^{*†}, T. Q. Donaghy^{*} and C. Graziani^{*}

^{*}*Department of Astronomy & Astrophysics, University of Chicago, Chicago, IL 60637*
[†]*d-lamb@uchicago.edu*

Abstract.

HETE-2 has provided strong evidence that the properties of X-Ray Flashes (XRFs) and GRBs form a continuum, and therefore that these two types of bursts are the same phenomenon. We show that both the structured jet and the uniform jet models can explain the observed properties of GRBs reasonably well. However, if one tries to account for the properties of both XRFs and GRBs in a unified picture, the uniform jet model works reasonably well while the structured jet model fails utterly. The uniform jet model of XRFs and GRBs implies that most GRBs have very small jet opening angles (\sim half a degree). This suggests that magnetic fields play a crucial role in GRB jets. The model also implies that the energy radiated in gamma rays is ~ 100 times smaller than has been thought. Most importantly, the model implies that there are $\sim 10^4 - 10^5$ more bursts with very small jet opening angles for every such burst we see. Thus the rate of GRBs could be comparable to the rate of Type Ic core collapse supernovae. Accurate, rapid localizations of many XRFs, leading to identification of their X-ray and optical afterglows and the determination of their redshifts, will be required in order to confirm or rule out these profound implications.

INTRODUCTION

Two-thirds of all HETE-2-localized bursts are either “X-ray-rich” or X-Ray Flashes (XRFs); of these, one-third are XRFs ¹ [20]. These events have received increasing attention in the past several years [6, 7], but their nature remains unknown.

XRFs have t_{90} durations between 10 and 200 sec and their sky distribution is consistent with isotropy. In these respects, XRFs are similar to “classical” GRBs. A joint analysis of WFC/BATSE spectral data showed that the low-energy and high-energy photon indices of XRFs are -1 and ~ -2.5 , respectively, which are similar to those of GRBs, but that the XRFs had spectral peak energies $E_{\text{peak}}^{\text{obs}}$ that were much lower than those of GRBs [7]. The only difference between XRFs and GRBs therefore appears to be that XRFs have lower $E_{\text{peak}}^{\text{obs}}$ values. It has therefore been suggested that XRFs might represent an extension of the GRB population to bursts with low peak energies.

Clarifying the nature of XRFs and X-ray-rich GRBs, and their connection to GRBs, could provide a breakthrough in our understanding of the prompt emission of GRBs. Analyzing 42 X-ray-rich GRBs and XRFs seen by FREGATE and/or the WXM instruments

¹ We define “X-ray-rich” GRBs and XRFs as those events for which $\log[S_X(2 - 30 \text{ keV})/S_\gamma(30 - 400 \text{ keV})] > -0.5$ and 0.0 , respectively.

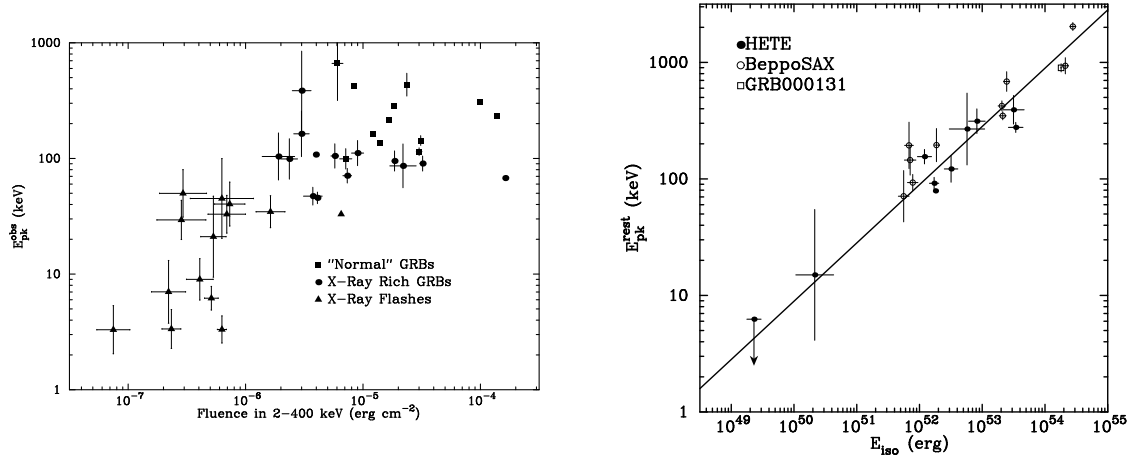


FIGURE 1. Distribution of HETE-2 bursts in the $[S(2-400 \text{ keV}), E_{\text{peak}}^{\text{obs}}]$ -plane, showing XRFs, X-ray-rich GRBs, and GRBs (left panel). From [20]. Distribution of HETE-2 and BeppoSAX bursts in the $(E_{\text{iso}}, E_{\text{peak}})$ -plane, where E_{iso} and E_{peak} are the isotropic-equivalent GRB energy and the peak of the GRB spectrum in the source frame (right panel). The HETE-2 bursts confirm the relation between E_{iso} and E_{peak} found by Amati et al. (2002), and extend it by a factor ~ 300 in E_{iso} . The bursts with the lowest and second-lowest values of E_{iso} are XRFs 020903 and 030723. From [10].

on HETE-2, [20] find that the XRFs, the X-ray-rich GRBs, and GRBs form a continuum in the $[S_{\gamma}(2-400 \text{ keV}), E_{\text{peak}}^{\text{obs}}]$ -plane (see Figure 1, left-hand panel). This result strongly suggests that all of these events are the same phenomenon.

Furthermore, [10] have placed 9 HETE-2 GRBs with known redshifts and 2 XRFs with known redshifts or strong redshift constraints in the $(E_{\text{iso}}, E_{\text{peak}})$ -plane (see Figure 1, right-hand panel). Here E_{iso} is the isotropic-equivalent burst energy and E_{peak} is the energy of the peak of the burst spectrum, measured in the source frame. The HETE-2 bursts confirm the relation between E_{iso} and E_{peak} found by [1] (see also [12]) for GRBs and extend it down in E_{iso} by a factor of 300. The fact that XRF 020903, one of the softest events localized by HETE-2 to date, and XRF 030723, the most recent XRF localized by HETE-2, lie squarely on this relation [19, 10] provides strong evidence that XRFs and GRBs are the same phenomenon. However, additional redshift determinations are clearly needed for XRFs with $1 \text{ keV} < E_{\text{peak}} < 30 \text{ keV}$ energy in order to confirm these results.

Figure 2 shows a simulation of the expected distribution of bursts in the $(E_{\text{iso}}, E_{\text{peak}})$ -plane (left panel) and in the $(F_N^{\text{peak}}, E_{\text{peak}})$ -plane (right panel), assuming that the [1] relation holds for XRFs as well as for GRBs [9], as is strongly suggested by the HETE-2 results. The SXC, WXM, and FREGATE instruments on HETE-2 have thresholds of 1–6 keV and considerable effective areas in the X-ray energy range. Thus HETE-2 is ideally suited for detecting and studying XRFs. In contrast, BAT on *Swift* has a nominal threshold of 20 keV. This simulation shows that the WXM and SXC instruments on HETE-2 detect many times more bursts with $E_{\text{peak}} < 10 \text{ keV}$ than will BAT on *Swift*.

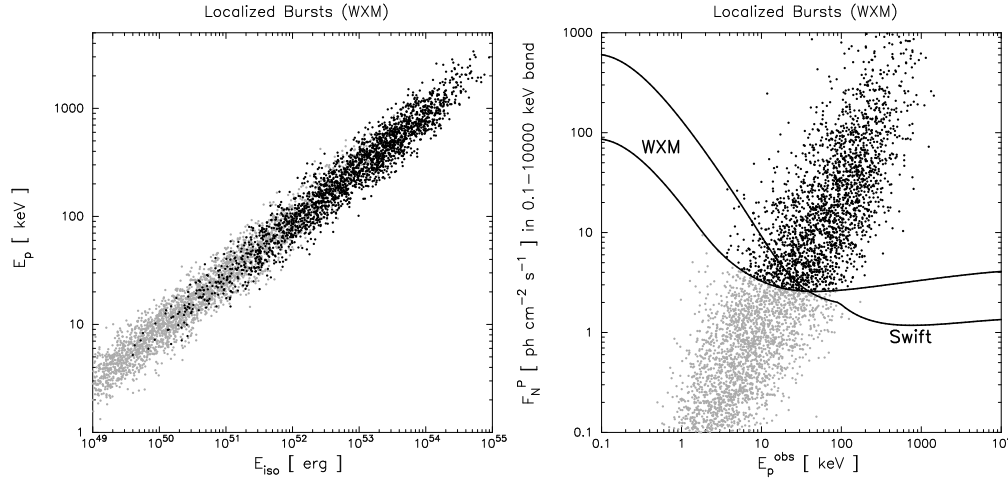


FIGURE 2. Expected distribution of bursts in the $(E_{\text{iso}}, E_{\text{peak}})$ -plane (left panel) and in the $(F_N^{\text{peak}}, E_{\text{peak}})$ -plane (right panel), assuming that the Amati et al. (2002) relation holds for XRFs as well as for GRBs, as strongly suggested by the HETE-2 results. Black dots are simulated bursts that the WXM on HETE-2 detects; gray dots are simulated bursts that it does not detect. The curved lines in the right-hand panel show the threshold sensitivities of the WXM on HETE-2 and BAT on Swift. From [9].

XRFs AS A PROBE OF GRB JET STRUCTURE, GRB RATE, AND CORE COLLAPSE SUPERNOVAE

Most GRBs have a “standard” energy [5, 15, 3]; i.e, if their isotropic equivalent energy is corrected for the jet opening angle inferred from the jet break time, most GRBs have the same radiated energy, $E_\gamma = 1.3 \times 10^{51}$ ergs, to within a factor of ~ 2 -3.

Two models of GRB jets have received widespread attention:

- The “structured jet” model (see the left-hand panel of Figure 3). In this model, all GRBs produce jets with the same structure [18, 22, 23, 14]. The isotropic-equivalent energy and luminosity is assumed to decrease as the viewing angle θ_v as measured from the jet axis increases. The wide range in values of E_{iso} is attributed to differences in the viewing angle θ_v . In order to recover the “standard energy” result [5], $E_{\text{iso}}(\theta_v) \sim \theta_v^{-2}$ is required [23].
- The “uniform jet” model (see the right-hand panel of Figure 3). In this model GRBs produce jets with very different jet opening angles θ_{jet} . For $\theta < \theta_{\text{jet}}$, $E_{\text{iso}}(\theta_v) = \text{constant}$ while for $\theta > \theta_{\text{jet}}$, $E_{\text{iso}}(\theta_v) = 0$.

As we have seen, HETE-2 has provided strong evidence that the properties of XRFs, X-ray-rich GRBs, and GRBs form a continuum, and that these bursts are therefore the same phenomenon. If this is true, it immediately implies that the E_γ inferred by [5] is too large by a factor of at least 100 [9]. The reason is that the values of E_{iso} for XRF 020903 [19] and XRF 030723 [10] are ~ 100 times smaller than the value of E_γ inferred by Frail et al. – an impossibility.

HETE-2 has also provided strong evidence that, in going from XRFs to GRBs, E_{iso} changes by a factor $\sim 10^5$ (see Figure 1, right-hand panel). If one tries to explain only

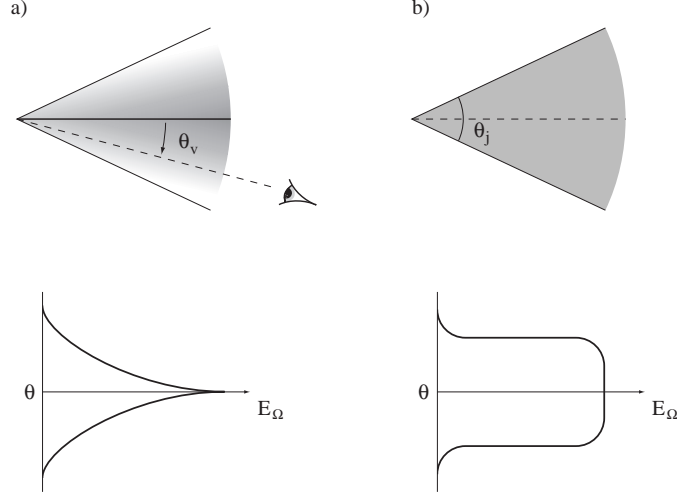


FIGURE 3. Schematic diagrams of universal jet model and jet model of GRBs [17]. In the universal jet model, the isotropic-equivalent energy and luminosity is assumed to decrease as the viewing angle θ_v as measured from the jet axis increases. In order to recover the “standard energy” result [5], $E_{\text{iso}}(\theta_v) \sim \theta_v^{-2}$ is required. In the uniform jet model, GRBs produce jets with a large range of jet opening angles θ_{jet} . For $\theta < \theta_{\text{jet}}$, $E_{\text{iso}}(\theta_v) = \text{constant}$ while for $\theta > \theta_{\text{jet}}$, $E_{\text{iso}}(\theta_v) = 0$.

the range in E_{iso} corresponding to GRBs, both the uniform jet model and the structured jet model work reasonably well. However, if one tries to explain the range in E_{iso} of a factor $\sim 10^5$ that is required in order to accommodate both XRFs and GRBs in a unified description, the uniform jet works reasonably well while the structured jet model does not.

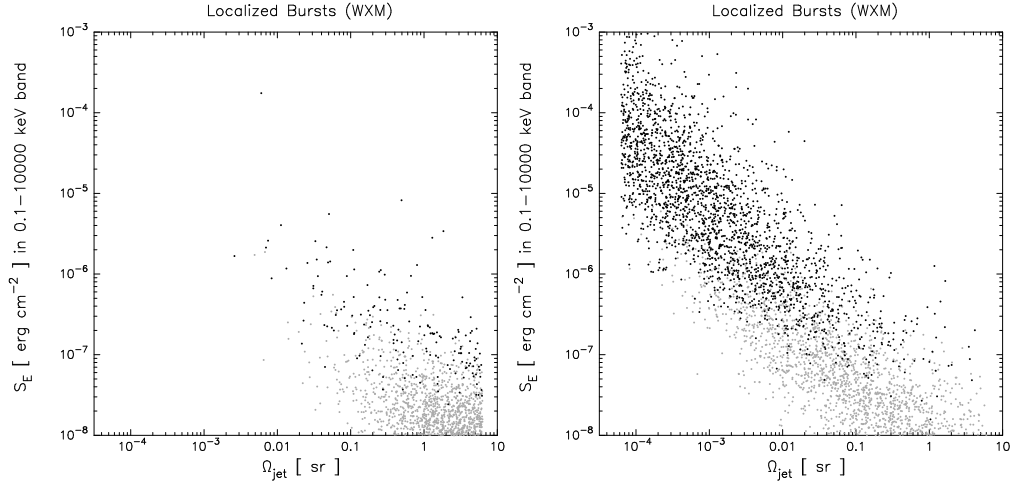


FIGURE 4. Expected distribution of bursts in the $(\Omega_{\text{jet}}, S_E)$ -plane for the universal jet model (left panel) and uniform jet model (right panel), assuming that the Amati et al. (2002) relation holds for XRFs as well as for GRBs, as the HETE-2 results strongly suggest. From [9].

The reason is the following: the observational implications of the structured jet model and the uniform jet model differ dramatically if they are required to explain XRFs and GRBs in a unified picture. In the structured jet model, most viewing angles θ_v are $\approx 90^\circ$.

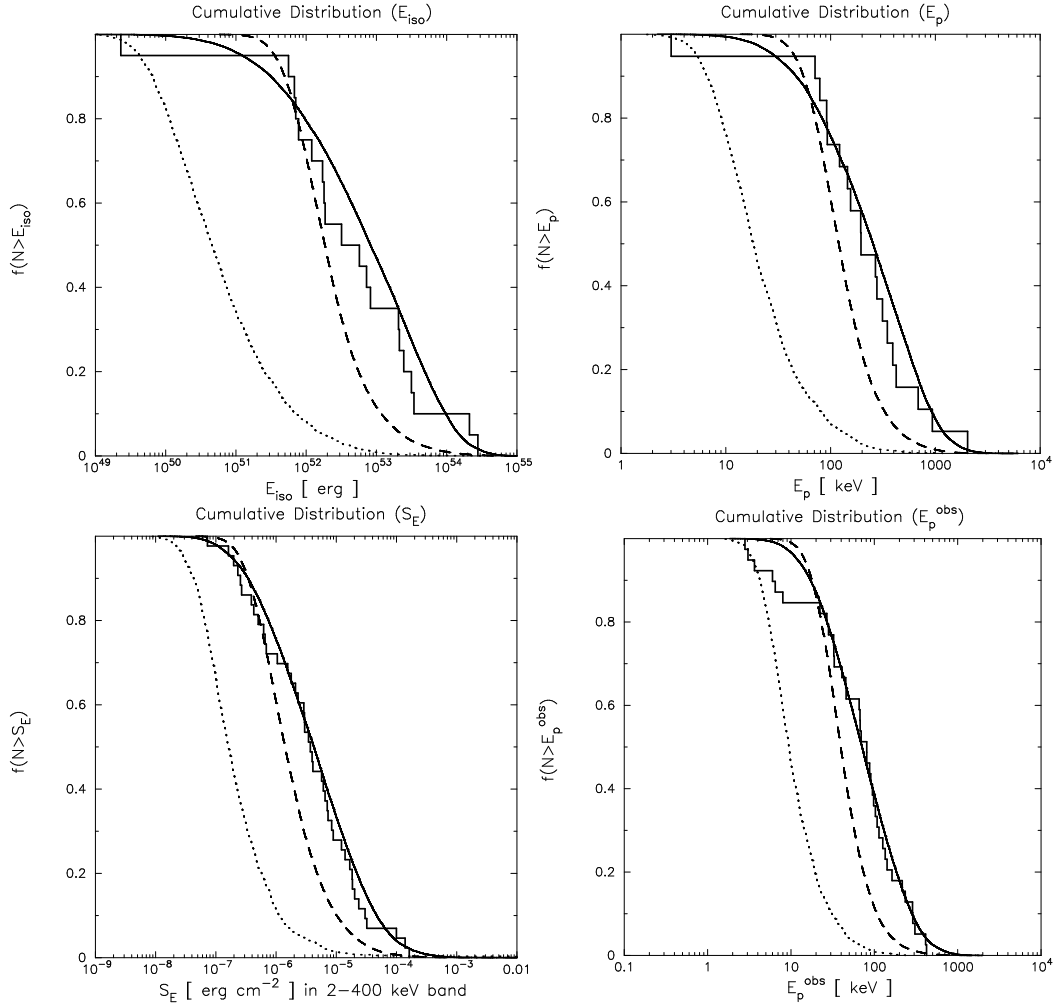


FIGURE 5. Top row: cumulative distributions of E_{iso} (left panel) and E_{peak} (right panel) predicted by various models, compared to the observed cumulative distributions of these quantities. Bottom row: cumulative distributions of $S(2-400\text{keV})$ (left panel) and $E_{\text{peak}}^{\text{obs}}$ (right panel) predicted by various models, compared to the observed cumulative distributions of these quantities. The uniform jet model is shown as a solid line. The cumulative distributions corresponding to the best-fit structured jet model that explains XRFs and GRBs are shown as dotted lines; the cumulative distributions corresponding to the best-fit structured jet model that explains GRBs alone are shown as dashed lines. The structured jet model provides a reasonable fit to GRBs alone but cannot provide a unified picture of both XRFs and GRBs, whereas the uniform jet model can. From [9].

This implies that the number of XRFs should exceed the number of GRBs by many orders of magnitude, something that HETE-2 does not observe (see Figures 1, 2, 4, and 5). On the other hand, by choosing $N(\Omega_{\text{jet}}) \sim \Omega_{\text{jet}}^{-2}$, the uniform jet model predicts equal numbers of bursts per logarithmic decade in E_{iso} (and S_E), which is exactly what HETE-2 sees (again, see Figures 1, 2, 4, and 5) [9]. Thus, if E_{iso} spans a range $\sim 10^5$, as the HETE-2 results strongly suggest, the uniform jet model can provide a unified picture of both XRFs and GRBs, whereas the structured jet model cannot. This means that XRFs provide a powerful probe of GRB jet structure.

A range in E_{iso} of 10^5 , which is what the HETE-2 results strongly suggest, requires a *minimum* range in $\Delta\Omega_{\text{jet}}$ of $10^4 - 10^5$ in the uniform jet model. Thus the unified picture of XRFs and GRBs in the uniform jet model implies that there are $\sim 10^4 - 10^5$ more bursts with very small Ω_{jet} 's for every such burst we see; i.e., the rate of GRBs may be ~ 100 times greater than has been thought.

In addition, since the observed ratio of the rate of Type Ic SNe to the rate of GRBs in the observable universe is $R_{\text{Type Ic}}/R_{\text{GRB}} \sim 10^5$ [8], a unified picture of XRFs and GRBs in the uniform jet model implies that the GRB rate is comparable to that of Type Ic SNe [9]. More spherically symmetric jets yield XRFs and narrow jets produce GRBs. Thus XRFs and GRBs provide a combination of GRB/SN samples that would enable astronomers to study the relationship between the degree of jet-like behavior of the GRB and the properties of the supernova (brightness, polarization \Leftrightarrow asphericity of the explosion, velocity of the explosion \Leftrightarrow kinetic energy of the explosion, etc.). GRBs may therefore provide a unique laboratory for understanding Type Ic core collapse supernovae.

A unified picture of XRFs and GRBs in the uniform jet model also implies that many Type Ic SNe produce narrow jets, which may suggest that the collapsing cores of many Type Ic supernovae are rapidly rotating. Finally, such a unified picture implies that the total radiated energy in gamma rays E_γ is ~ 100 times smaller than has been thought [9].

REFERENCES

1. Amati, L., et al. 2002, A & A, 390, 81
2. Band, D. L. 2003, ApJ, in press (astro-ph/0212452)
3. Bloom, J., Frail, D. A. & Kulkarni, S. R. 2003, ApJ, 588, 945
4. Fox, D. W., et al. 2003c, GCN Circular 2323
5. Frail, D. et al. 2001, ApJ, 562, L55
6. Heise, J., in't Zand, J., Kippen, R. M., & Woods, P. M., in Proc. 2nd Rome Workshop: Gamma-Ray Bursts in the Afterglow Era, eds. E. Costa, F. Frontera, J. Hjorth (Berlin: Springer-Verlag), 16
7. Kippen, R. M., Woods, P. M., Heise, J., in't Zand, J., Briggs, M.S., & Preece, R. D. 2002, in Gamma-Ray Burst and Afterglow Astronomy, AIP Conf. Proc. 662, ed. G. R. Ricker & R. K. Vanderspek (New York: AIP), 244
8. Lamb, D. Q. 1999, A&A, 138, 607
9. Lamb, D. Q., Donaghy, T. Q., & Graziani, C. 2003, ApJ, submitted
10. Lamb, D. Q., et al. 2003, ApJ, submitted
11. Lazzati, D., Ramirez-Ruiz, E. & Rees, M. J. 2002, ApJ, 572, L57
12. Lloyd, N. M., Petrosian, V. & Mallozzi, R. S. 2000, ApJ, 534, 227
13. Lloyd-Ronning, N., Fryer, C., & Ramirez-Ruiz, E. 2002, ApJ, 574, 554
14. Mészáros, P., Ramirez-Ruiz, E., Rees, M. J., & Zhang, B. 2002, ApJ, 578, 812
15. Panaitescu, A. & Kumar, P. 2001, ApJ, 556, 1002
16. Prigozhin, G., et al. 2003, GCN Circular 2313
17. Ramirez-Ruiz, E. & Lloyd-Ronning, N. 2002, New Astronomy, 7, 197
18. Rossi, E., Lazzati, D., & Rees, M. J. 2002, MNRAS, 332, 945
19. Sakamoto, T. et al. 2003a, ApJ, in press
20. Sakamoto, T. et al. 2003b, ApJ, to be submitted
21. Soderberg, A. M., et al. 2002, GCN Circular 1554
22. Woosley, S. E., Zhang, W. & Heger, A. 2003, ApJ, in press
23. Zhang, B. & Mészáros, P. 2002, ApJ, 571, 876